Probes of membrane electrostatics: synthesis and voltage-dependent partitioning of negative hydrophobic ion spin labels in lipid vesicles

J. Craig Franklin,* David S. Cafiso,* Ross F. Flewelling,‡ and Wayne L. Hubbell‡

*Department of Chemistry and Biophysics Program, University of Virginia, Charlottesville, Virginia 22901; and ‡Jules Stein Eye Institute and the Department of Chemistry and Biochemistry, University of California, Los Angeles, California 90024 USA

ABSTRACT Two spin-labeled derivatives of the hydrophobic anion trinitrophenol have been synthesized and characterized in lipid vesicles. In the presence of lipid vesicles, the electron paramagnetic resonance (EPR) spectra of these probes are a composite of both membrane-bound and aqueous populations; as a result, the membrane-aqueous partitioning can be determined from their electron paramagnetic resonance spectra. The effect of transmembrane potentials on the membrane-aqueous partitioning of these spin-labeled hydrophobic ions was examined in phosphatidylcholine vesicles formed by extrusion. Inside positive membrane potentials promote an increase in the binding of these probes that is quantitatively accounted for by a simple thermodynamic model used previously to describe the partitioning of paramagnetic phosphonium ions. The transmembrane migration rates of these ions are dependent on the dipole potential, indicating that these ions transit the membrane in a charged form. The partitioning of the probe is also sensitive to the membrane surface potential, and this dependence is accurately accounted for using the Gouy-Chapman Stern formalism. As a result of the membrane dipole potential, these probes exhibit a stronger binding and a more rapid transmembrane migration rate compared with positive hydrophobic ion spin labels and provide a new set of negatively charged hydrophobic ion probes to investigate membrane electrostatics.

INTRODUCTION

Membrane electrostatic potentials are known to play a role in processes such as membrane excitability, the binding of extrinsic proteins to membrane surfaces (1), the insertion of membrane active toxins and the folding of membrane proteins during synthesis (2–5). At the present time, the molecular basis for these voltage-dependent processes are largely uncharacterized, and a number of fundamental questions remain to be answered regarding membrane electrical properties.

Fig. 1 is a schematic representation of the electrostatic potentials across a phospholipid bilayer that arise from the separation of fixed charges and/or oriented dipoles. The transmembrane potential ($\Delta\psi$) arises from the separation of net charge across the entire thickness of the bilayer; the surface electrostatic potentials (ψ_s) arise from charges fixed at the membrane solution interface, and dipole potentials (ψ_d) have contributions from oriented dipoles on the phospholipids and/or water molecules (6–11). It is the interaction of protein charges and dipoles with these potentials that gives rise to the voltage-dependent phenomena mentioned above. For example, the adsorption of extrinsic proteins will be strongly influenced by the surface potentials, whereas the energetics of insertion into the membrane interior will have important contributions from both the dipole and transmembrane potentials. Conversely, the interaction of charged or dipolar proteins with the bilayer can modulate these potentials. For example, conformational changes of membrane proteins that lead to intramembrane charge displacement can produce changes in the dipole potential and transmembrane potential. Such electrically active conformational changes have been described in voltage-gated ion channels and the photoreceptor protein rhodopsin (12).

Thus, it is important to develop strategies to estimate these microscopic membrane potentials as a means of investigating voltage-dependent phenomena. One important molecular tool for the characterization of membrane electrostatic properties is the hydrophobic ion. Hydrophobic ions are unusual among charged species in that they readily enter the interior of biological membranes (13–16). This property can be understood by considering the free energy profiles for hydrophobic ions across membranes. In the absence of surface potentials, the total free energy of transferring a hydrophobic ion from solution to a given position in the membrane can be approximated as

$$\Delta G^0 = \Delta G^0_{\text{Born}} + \Delta G^0_{\text{Dipole}} + \Delta G^0_{\text{Hydro}},$$

where ΔG_{Born} is the (repulsive) electrostatic "image" energy, ΔG_{Hydro} is the (attractive) hydrophobic energy, and ΔG_{Dipole} is the energy of interaction with membrane dipolar fields of structural origin (17). Fig. 2 *A* shows schematically these individual contributions to the overall free energy profile, and Fig. 2 *B* shows the total free energy for both a cationic and an anionic hydrophobic ion. The Born image energy is large and positive for all ions, positive or negative, and is responsible for the low permeability of membranes to ions in general. This energy is inversely proportional to the ionic radius, and larger ions are thus more permeable. In the case of large and hydrophobic ions, the size effect and the hydrophobic energy

Address correspondence to either Dr. Cafiso or Dr. Hubbell.

Ross F. Flewelling's present address is Nellcor, Inc., 25495 Whitesell St., Hayward, CA 94545.

0006-3495/93/03/642/12 $2.00

act to overcome the Born energy to a large extent and the ion can readily enter the membrane interior. As shown in Fig. 2, the summation of the individual energy terms gives rise to a free energy minimum near the membrane/solution interface corresponding to a "binding" site. The potential at this binding site is sometimes referred to as a "boundary" potential (6, 15).

As a result of these properties, hydrophobic ions are distributed throughout all spatial domains in a membrane system. In the presence of electrostatic potentials such as those shown in Fig. 1, the equilibrium spatial distribution of hydrophobic ions will be influenced by the magnitude and sign of the various potentials. Thus, if a method was available for determining the distribution of a hydrophobic ion in a membrane, then the electrostatic potentials and their changes could be determined relative to a reference state. This strategy has met with considerable success using electron paramagnetic resonance (EPR) spectroscopy to determine the distribution of spin-labeled hydrophobic ions. For example, spin-labeled phosphonium ions have been used to investigate transmembrane, surface, and dipole potentials in pure bilayers and have been used to detect transient changes in boundary potential during photo excitation in photoreceptor membranes (18).

It is generally agreed that the rate constant for membrane transport is determined by the maximum in the free energy profile near the center of the membrane. As shown in Fig. 2, this maximum arises primarily from the Born image energy but apparently has an important contribution from the energy of interaction with the dipole potential that is of opposite sign for cations and anions (Fig. 2). This accounts for the experimentally observed fact that otherwise similar cations and anions can have as much as a 10^6 times difference in transport rate constant (19). There are two points to be made regarding these features of hydrophobic ions that pertain to their use as spin-label probes of membrane potentials. First, a cationic probe will have a relatively slow equilibration rate across membranes and will thus have limited time resolution for following time-varying potentials. Clearly, an anionic probe would be preferred for such studies. Second, a comparison of the transmembrane flux for a cation and anion under identical conditions can give information on the electrostatic potentials near the center of the membrane, information that could not be obtained from a study of the equilibrium distribution of the ions because of their low concentration in this region. Finally, anionic probes can be used to determine positive-inside transmembrane potentials, a situation where the phosphonium spin labels are of little use (20). For these reasons, it is highly desirable to develop anionic hydrophobic ions as probes of membrane electrostatic potentials to complement the existing phosphonium spin labels, and that is the subject of the present article.

The synthesis and characterization of two new spin-labeled hydrophobic anion probes are described. These probes, I and II shown below, are based on the hydrophobic anion, trinitrophenolate (TNP) (21). They exhibit a voltage-dependent aqueous-membrane phase

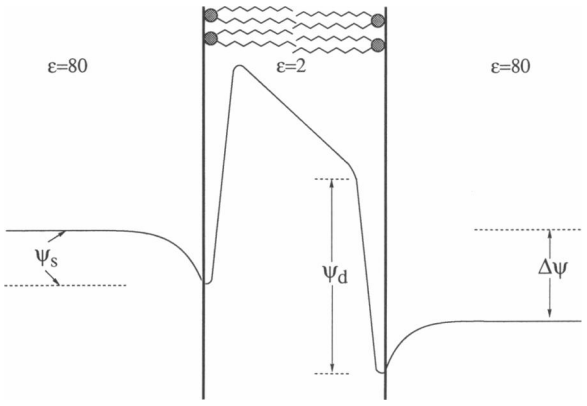

FIGURE 1 Electrostatic potentials across phospholipid bilayers. The surface potential ψ_s arises from charged groups that are associated with the membrane interface. The transmembrane potential $\Delta\psi$ results from the net separation of charge across the membranes, and ψ_d is the membrane dipole potential. ψ_d is a large hydrocarbon positive potential that arises from a molecular dipole layer at the membrane-solution interface.

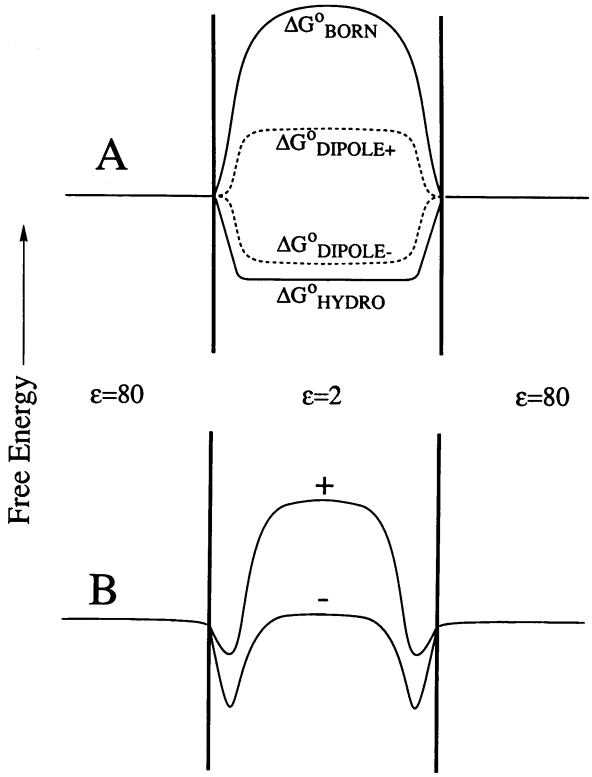

FIGURE 2 Free energy profiles of hydrophobic ions across phospholipid bilayers. (*A*) Individual energy contributions, which include the dipole energy ($\Delta G^0_{\text{Dipole}}$), the attractive hydrophobic energy ($\Delta G^0_{\text{Hydro}}$), and the strongly repulsive electrostatic charging energy (ΔG^0_{Born}). (*B*) Total free energy profiles for a hydrophobic anion and cation that are the sums of the energy terms shown in *A*.

partitioning that can be described accurately by a thermodynamic analysis used previously to describe the partitioning of hydrophobic phosphonium probes (20). Unlike the phosphoniums, the TNP probe I exhibits a rapid transmembrane equilibration rate with a half-time of <10 ms. Thus, I will be useful in following rapid charge displacements in membranes, such as the movement of gating charges in voltage-dependent channels. Probe II has a slow transmembrane equilibration rate, similar to the phosphoniums previously described, and the transmembrane flow can be monitored readily with conventional EPR stopped-flow instrumentation (22, 23). Comparison of the flux of II with that of phosphoniums will be useful in deducing the electrostatic barrier to transport and how it is effected by membrane proteins.

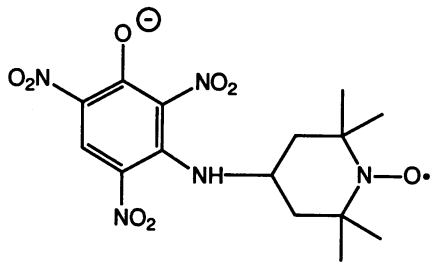

I

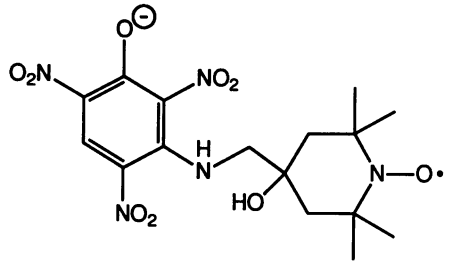

II

EXPERIMENTAL

Materials

Egg phosphatidylcholine (EPC) was isolated from fresh hen eggs according to the procedure of Singleton et al. (24) and was stored in chloroform solution at −20°C. 1,3, Dichloro-2,3,5 trinitrobenzene (DCTNB) was a gift of Chemtronix, Inc. (Swannanoa, NC). The nitroxides 4-amino tempo and 4-oxo tempo were obtained from Aldrich Chemical Co. (Milwaukee, WI)

Formation of lipid vesicles

Electrical measurements were made in lipid vesicles formed from EPC. Lipid vesicle suspensions were prepared by measuring out the appropriate aliquot of the lipid chloroform solution, removing the solvent under a stream of argon, and drying the lipid overnight in a vacuum desiccator. The appropriate buffer solutions were added to the lipid (see below), and the suspension was vortexed and freeze-thawed five times using liquid nitrogen. The lipid-buffer mixture was extruded 10 times through 0.05-μm polycarbonate filters using a commercially available unit (Lipex Biomembranes Inc., Vancouver, BC). The vesicle suspension was centrifuged at 13,000 g for 30 min to remove small amounts of nonvesicular lipid. In all cases, except those involving phosphatidylserine, the pH of the extruded vesicles suspension did not differ from that of buffer used to hydrate the lipid initially. The phospholipid concentrations in the final vesicle suspension were determined using a modified Fiske-Subbarrow phosphate assay (25).

Generation of membrane potentials

To form transmembrane potentials, pH gradients were established across lipid vesicles and protons were brought to electrochemical equilibrium using a protonophore. In these experiments, the buffer used to hydrate the lipid contained 100 mM 2-{[tris- (hydroxymethyl)-methyl]-amino} ethanesulfonic acid and was adjusted to an osmotic strength of 154 mM with Na_2SO_4 using a vapor pressure osmometer. After formation of the lipid vesicles by extrusion, the external pH was adjusted to a more acidic value by diluting the vesicle suspension with an equal volume of an isoosmotic solution containing one of the following buffers: 3-(N-morpholino)-propane-sulfonic acid, pH = 7.0, osmolarity = 153 mM; N-(2-acetamido)-2-aminoethane-sulfonic acid (ACES), pH = 6.5, osmolarity = 150 mM; 2-(N-morpholino)-ethanesulfonic acid, pH = 6.0 and pH = 5.5, osmolarity = 156 and 155 mM. The osmolarity was adjusted by the addition of Na_2SO_4. To prevent electrostatic saturation of the probe binding (19), 5-μM spin-labeled TNP was used with a lipid concentration of 0.385 mg/ml. To bring protons to electrochemical equilibrium and generate an inside positive potential, 300 nM carbonyl cyanide m-chloro-phenylhydrozone (CCCP) was added to the vesicle suspension. As described previously, the transmembrane equilibration of protons and probe can diminish the magnitude of the potential expected based on the initial proton gradient (26). Although this correction is small (<5%), the expected potentials can be obtained by solving for $f(x) = 0$ (Eq. 1), where $x \equiv [H^+]_{in}/[H^+]_{out}$, $\Delta\psi = -(RT/F) \ln x$, and:

$$f(x) = \left(\frac{RT}{F}\right) \ln(x) + \left(\frac{c}{e}\right)\left[\frac{V_i K_a C_B (x[H^+]^i_{out} + [H^+]^i_{in})N}{(K_a + [H^+]^i_{in})(K_a + x[H^+]^i_{out})} + \frac{N_T}{1 + (V_o/V_i)(\epsilon_o/\epsilon_i)(1/x)}\right]. \quad (1)$$

Here, e is the electronic charge, c is the membrane specific capacitance (which will be taken as 0.9 μFd/cm^2) (27), N is Avogadro's number, and C_B is the buffer concentration. The initial concentrations on the inside and outside of the vesicle are indicated by a superscript i, and N_T is the total number of probe molecules per vesicles. In this expression, $\epsilon_i \equiv 1 + KV_{mi}/V_i$ and $\epsilon_o \equiv 1 + KV_{mo}/V_o$, where K is the binding constant for the probe on each vesicle surface, and V_o, V_i, V_{mo}, V_{mi} are the effective thermodynamic volumes occupied by probe in the external and internal aqueous spaces and the external and internal membrane binding domains, respectively.

To establish surface potentials, phosphatidylserine (PS) (Avanti Polar Lipids, Birmingham, AL), dissolved in chloroform, was added to EPC at 10, 20, and 30 mol% PS. The lipid mixture was dried and hydrated in 5 mM ACES, 100 mM NaCl buffer, and extruded as described above. After vesicle formation, the pH showed a slight downward shift. Steps were taken in subsequent manipulations to ensure that no pH gradient or potentials were present when the EPR spectra were obtained. The procedure outlined above for determining binding constants was used for each PS-EPC mixture.

EPR spectroscopy

EPR spectroscopy was carried out either on a Bruker (Billerica, MA) ESP 300 EPR spectrometer or a Varian (Sunnyvale, CA) E-Line Century series spectrometer. Typically, the spectra were obtained at a mod-

ulation amplitude of 1 G (p − p) with an incident microwave power of 10 mW. To reproducibly obtain binding data for these probes, a large quartz sample cell (300 μl) was fitted to the EPR cavity that allowed additions of probe or lipid without the need to remove the cell from the cavity. To a solution containing 5 μM of I, measured amounts of lipid were added to the solution and the spectra recorded. The resulting series of spectra were used to obtain a binding curve.

As described previously, the EPR spectra of nitroxides that partition to membranes provide a direct measure of the ratio of membrane associated to aqueous spins (18). Briefly, the intensity of the high-field resonance line provides a measure of the spin probe in aqueous solution. By calibrating this signal with a sample of known spin concentration, the ratio of the bound to free spin label, λ, can be determined according to:

$$\lambda = \frac{Nb}{Nf} = \frac{A_f^0 - A}{A - (b/a)A_f^0}, \qquad (2)$$

where A is the amplitude of the $m_I = -1$ resonance in the presence of membranes and A_f^0 is the amplitude of the $m_I = -1$ nitroxide resonance in the absence of membranes. The constants a and b are proportionality constants that relate the $m_I = -1$ amplitude of the bound and free signals, respectively, to the number of bound or free spins. Because the lineshape of the $m_I = -1$ resonance for the bound spin is usually broad, b/a is usually small. Probes I and II have very broad bound lineshapes (see below), and b/a was taken as 0.

Spectral simulations were done with the program EPRLF generously provided by Freed and co-workers (28, 29), and experimental spectra were fit using a least-squares procedure. Starting values for the Euler angles relating the magnetic tensor to the diffusion tensor were taken from energy minimized models of the spin labels I and II. Energy minimization of the structures was carried out using InsightII and Discover (Biosym Technologies, San Diego, CA)

Synthesis of I

DCTNB (198 mg; 0.7 mM) was dissolved in a minimal amount of freshly distilled tetrahydrofuran (THF) and added to a solution of dry 4-amino-tempo (120 mg; 0.7 mM) in a minimal amount of freshly distilled methanol at 0°C. The mixture was allowed to come to room temperature and stirred for 6 h. After removing the solvent by rotary evaporation, the product mixture was purified on a silica flash column (Baker, Instruments, Bethlehem, PA; silica for flash chromatography) using hexane:ethyl acetate 6:1 (see Still et al. (30) for a description of the flash technique). The first major fraction off the column was collected, dissolved in freshly distilled dioxane, and five equivalents of dry powered KOH were added to hydrolyze the active chlorine. The course of the hydrolysis was followed by measuring the absorption of light at 340 and 410 nM. Over an 8-h period, the 340:410 ratio changed from 2.2 to 1.1 and was judged complete when the ratio remained constant for 4 h. The mixture separated into three major fractions on a 2-cm-diameter silica flash column using hexane:ethyl acetate 1:3. The second fraction was collected and further purified by high performance thin layer chromatography (HPTLC). Approximately 3 mg of the second major product was loaded onto an analytical HPTLC plate (Merck, Darmstadt, Germany; Silica Gel 60) and was concentrated into a narrow band with ethyl acetate. The major band (rf = 0.6) after being developed in hexane:ethyl acetate, 1:3, was removed from the plate, and the silica was washed with ethyl acetate. The major spot was recovered yielding 2.4 mg of a water soluble product with a nitroxide signal consistent with the expected molecular weight. High-resolution mass spectrometry revealed a cation molecular weight of 397, consistent with the expected molecular weight of 398.

Synthesis of II

Probe II was synthesized by the following reaction scheme:

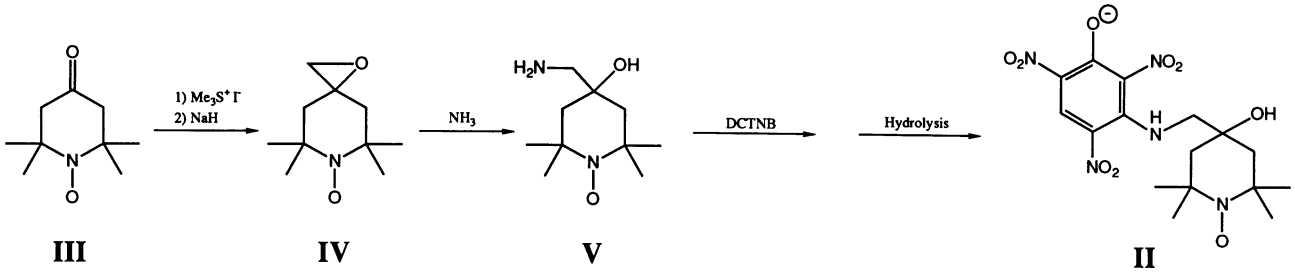

The epoxide IV was prepared from the ketone III as shown following a procedure given by Corey and Chaykovsky (31) and purified according to Rauchman et al. (32). The amino alcohol V was prepared using a procedure similar to that described by McManus et al. (33). Briefly, 871.6 mg (4.737 mM) of IV was placed in a stainless steel bomb and cooled in a dry ice acetone bath to which 500 μl of water had been added. Approximately 50 ml of liquid ammonia was slowly poured into the bomb, the bomb valve was closed, and then placed in a 5 gallon water bath that had been preheated to 75°C. After 90 min, the bomb was cooled in a dry ice acetone bath and opened. The bomb was warmed to room temperature to allow excess ammonia to evaporate. The reaction mixture was separated on a 2.5-cm flash column running a gradient that ranged from CH_3CN to CH_3CN:MeOH (10:1). The desired product, V, was the last of three components that eluted, and a total of 0.74 gm was obtained. The identity of V was confirmed by its positive reaction with ninhydrin, an EPR signal of appropriate magnitude, the presence of a strong infrared absorption around 3,000 cm^{-1} corresponding to hydroxy and amine functionality, and an m/z value of 201 by mass spectrometry.

To produce the spin label II, 690 mg (3.4 mM) of V dissolved in methanol was added slowly to 2 g (7.14 mM) of DCTNB and 480 μl (3.44 mM) of triethylamine (TEA), stirring in THF. The reaction was followed with thin layer chromatography (TLC) (hexane:ethyl acetate 3:1) and appeared to be 75% complete after 18 h. The pure material (639 mg) was recovered after chromatography on a 2.5-cm silica gel flash column eluting with hexane:ethyl acetate 3:1. The infrared spectrum yielded the expected amine doublet at 3,000 cm^{-1} and aromatic resonances at 1,240, 1,260, 1,270, and 1,300 cm^{-1}. Negative and positive ion chemical ionization mass spectrometry (CI MS) measured an m/z value of 446.

The hydrolysis of 1-chloro-3-β-OH TEMPO-2,4,6-trinitrobenzene was carried out by adding five equivalents of powdered KOH to 640 mg of the product dissolved in dioxane. On the addition of ~3 ml of water used to dissolve the KOH, the solution turned a deep red. The solution was allowed to stand at room temperature for several hours and was then raised to 40°C for 1 h. The reaction was judged to be complete as determined by TLC and the 340:410 absorbance ratio. The product mixture was dried by rotary evaporation, dissolved in a minimal amount of water, and extracted into chloroform. The product was resolved to a single peak using HPLC with programmed gradient of 100%

H_2O for 10 min to 90% H_2O:10% CH_3CN over 30 min, followed by isocratic 90% H_2O:10% CH_3CN. The peak eluted in 53 min using a flow rate of 3 ml/min on a Vydac reverse phase C18 column. Positive and negative ion fast atom bombardment mass spectrometry (FAB MS) of this product yielded a value for m/z of 428.

RESULTS

Trinitrophenol nitroxides exhibit a voltage-dependent phase partitioning

The spin-labeled trinitrophenol derivatives I and II were synthesized with the expectation that they would exhibit a voltage-dependent binding in lipid vesicle systems. Shown in Fig. 3 *B* are two superimposed spectra recorded for probe I in the presence of lipid vesicles with and without a transmembrane potential. The changes seen in these spectra on application of an inside positive membrane potential are qualitatively similar to those seen previously for spin-labeled hydrophobic cations (with the application of an inside negative potential). The high-field resonance of I is dramatically diminished in the presence of a potential and is the result in a change in the membrane aqueous partitioning of the probe.

The thermodynamic parameters that govern the binding and voltage-dependent phase partitioning of I and II have been determined and are described below. These parameters are used along with a thermodynamic model to predict the partitioning of the probe as a function of the membrane potential. This predicted behavior is then compared with the experimentally determined probe partitioning at several membrane potentials and used to establish the mechanism by which these probes function.

Spin-labeled hydrophobic anions strongly associate with lipid bilayers

The EPR spectra of nitroxide probes I or II in aqueous solution yield sharp isotropic resonances similar to the spectra obtained for other water soluble nitroxides (Fig. 3 *A*). In the presence of lipid vesicles, the spectra are a composite of an isotropic signal due to an aqueous population of probe and a broadened signal due to a more slowly reorienting membrane associated population (Fig. 3 *C*). This bound population corresponds to nitroxides occupying the free energy minima shown in Fig. 2 *B*. Fig. 4 shows the EPR spectral lineshapes of I and II bound to vesicles in the absence of a potential. Although the molecules only differ by the presence of a $-CH_2OH$ group, these spectra are distinct and suggest different motions in the membrane binding site. Both spectra can be reasonably well simulated, assuming axially symmetric diffusion tensors with the unique axes parallel to the long molecular axes of I and II. Fig. 5 shows energy minimized models of I and II together with the unique diffusion axis required for a good fit between experimental and simulated spectra. The simulated spectra are shown in Fig. 4 immediately below their experimental spectra. The magnetic parameters derived from the simulation indicate that I undergoes very rapid axial rotation ($\tau_\parallel$ =

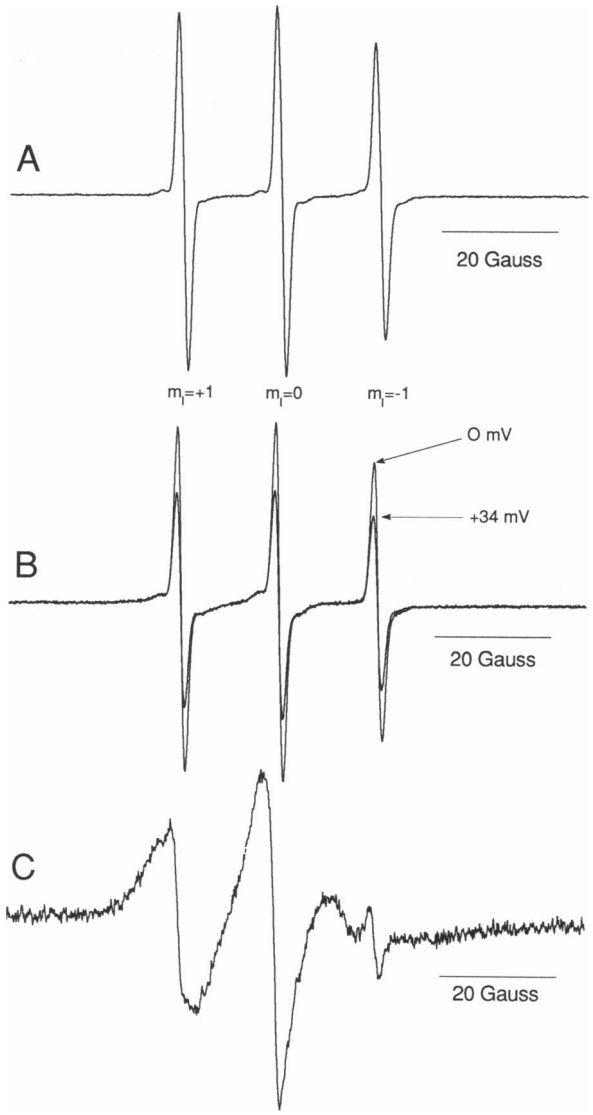

FIGURE 3 EPR spectra of II. (*A*) 20 μM II in solution; (*B*) 20 μM II in the presence of lipid vesicles (0.74 mg/ml) with and without a transmembrane potential of 34 mV inside positive. The decrease in the signal intensity of the spectra in the presence of a potential is due to an increase in the phase partitioning of the probe to the membrane phase. The potential is produced in this case by the addition of ~0.1 μM CCCP to a sample that has an initial pH gradient of +0.64 (see text); (*C*) the spectrum of II bound to phospholipid vesicles was obtained by the addition of 20 μM II to lipid vesicles at a lipid concentration of (46 mg/ml). A small signal arising from aqueous label is also present.

0.2 ns) with a slow motion about the perpendicular axis ($\tau_\perp$ = 200 ns). The A tensor values indicate that the nitroxide on I is located in a polar environment (A_{iso} = 16.7 G) in the membrane bound state, consistent with the interfacial location suggested by the position of the minima in Fig. 2.

For II, the simulation parameters indicate that the molecule undergoes an order of magnitude slower axial rotation rate than I ($\tau_\parallel$ = 2 ns), suggesting that the hydroxyl group on II is involved in hydrogen bonding to the lipid headgroups. In addition, the rotation rate about the per-

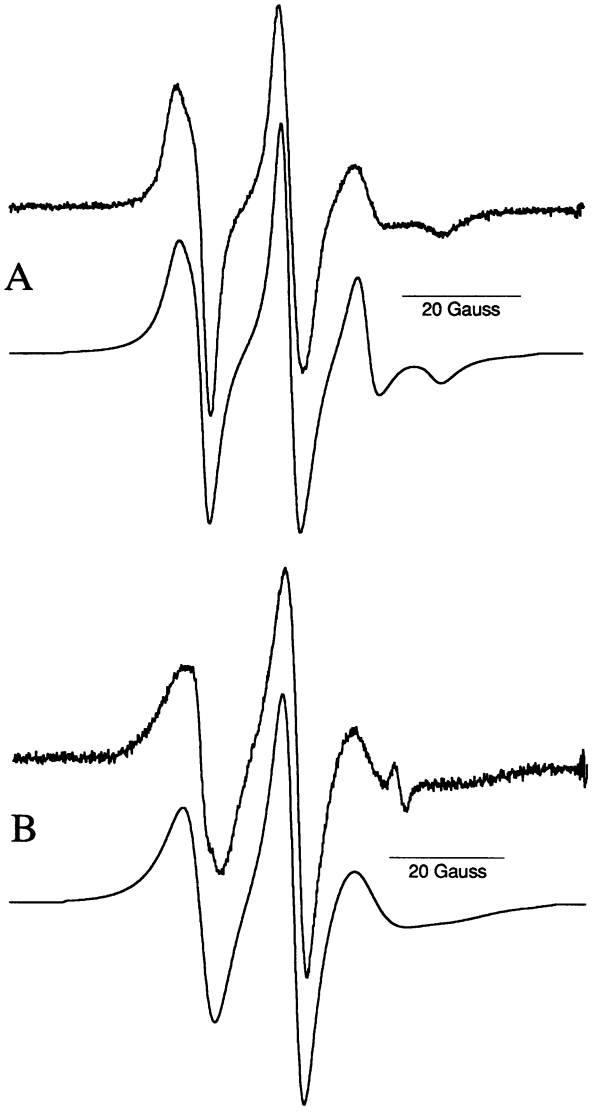

FIGURE 4 Experimental and simulated EPR spectra of I and II bound to phospholipid bilayers. The computed spectra were obtained by least-squares fitting of the experimental spectra as described in Experimental. The principle elements of the g tensor were fixed at g_{xx} = 2.00890, g_{yy} = 2.00613, g_{zz} = 2.00238 (50). The principle elements of the A tensor, the two rotational diffusion constants, and the Euler angles α and β defining the diffusion tensor were treated as adjustable parameters. The Euler angle γ was fixed at 0° (for definitions of the quantities and a general discussion of spectral simulation, see reference 29). Note below that the magnetic parameters for the two molecules are very similar, and they differ primarily in the geometry and rates of motion. (*A*) The experimental (above) and computed spectra for I in bilayers. The best fit parameters were A_{xx} = 7.87, A_{yy} = 6.55, A_{zz} = 35.69, α = 89°, β = 41.8°, $R_{\parallel}$ = 7.1 × 10^8 s^{-1}, and $R_{\perp}$ = 1.2 × 10^6 s^{-1}. (*B*) The experimental (above) and computed spectra for II in bilayers. The best fit parameters were A_{xx} = 8.19, A_{yy} = 6.71, A_{zz} = 34.48, α = 23°, β = 74.4°, $R_{\parallel}$ = 7.6 × 10^7 s^{-1}, and $R_{\perp}$ = 4.0 × 10^7 s^{-1}.

pendicular axis is much greater than for I ($\tau_{\perp}$ = 4 ns), perhaps due to the polar hydroxyl group making transient excursions to the surface.

From the composite EPR spectra of I and II in the presence of vesicles, the binding constant of the probes

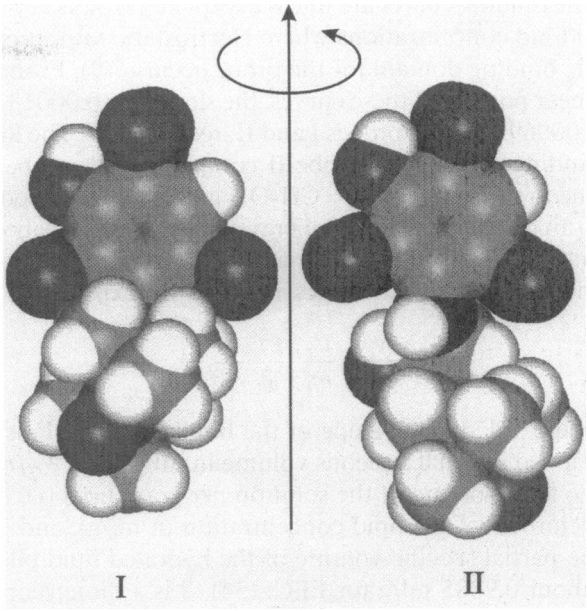

FIGURE 5 Molecular models of I and II showing the unique diffusion axis used in spectral simulation. The symmetry axis for diffusion coincides with the long molecular axis defined by geometry. The 2p orbital on nitrogen makes a greater angle with the rotation axis in II than in I, consistent with the relative values of the Euler angle β (74.1 and 40.4°, respectively) required for good spectral simulation.

to lipid vesicles formed from EPC was determined (see Eq. 2 above) and is plotted in Fig. 6. Here the ratio of aqueous to membrane bound probe N_f/N_b (or $1/\lambda$) is plotted versus V_T/ml (the total volume per gram lipid).

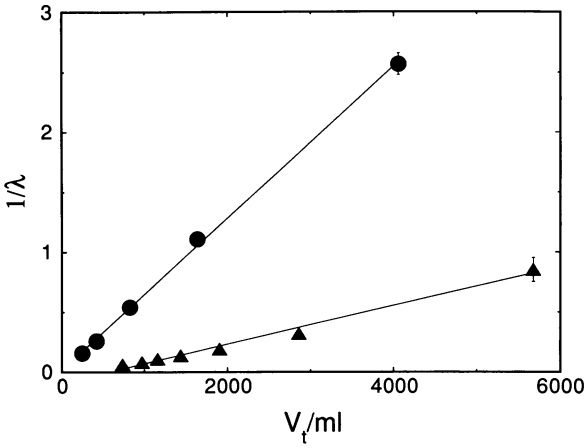

FIGURE 6 A plot of V_T/ml, the reciprocal of the lipid concentration in milliliters/gram, versus the ratio Nf/Nb ($1/\lambda$) for probes I (▲) and II (●) at a pH of 6.8. These binding curves to PC vesicles yield a slope that is linear at high lipid to probe ratios. This slope is given by $1/Vi\beta$, where β is directly related to the binding constant (see text). The values of β are 7,810 and 1,477 for I and II, respectively. Assuming that these probes occupy a binding domain that is 4-Å wide, binding constants of 19.2 × 10^3 and 3,600 are obtained for I and II, respectively. This difference in binding constant between I and II corresponds to a difference in the free energy of binding of ~1 kcal/mol.

The binding curves are linear except at the highest probe to lipid concentrations where electrostatic saturation of the binding domain for the probe occurs (19). From the linear portion of these curves, the slopes are 0.00013 and 0.00069 g/ml for probes I and II, respectively. The lower binding constant of probe II compared with probe I is due to the additional $-CH_2OH$ group and corresponds to an increase in the free energy of partitioning of about 1 kcal/mol. As shown previously, the binding curves shown in Fig. 6 can be described by the expression:

$$\frac{N_f}{N_b} = \frac{V_T}{m_l}\frac{1}{\bar{V}_i\beta} - \frac{1}{\beta}\frac{\bar{V}_l}{\bar{V}_i}, \quad (3)$$

where $1/V_i\beta$ is the slope of the binding curve, V_i is the trapped internal aqueous volume in ml/g lipid, V_T/ml is the total volume of the solution per gram lipid (i.e., the reciprocal of the lipid concentration in ml/g), and V_l is the partial specific volume of the hydrated lipid bilayer (about 0.9885 ml/g for EPC) (34). β is a dimensionless parameter defined by $\beta = K_oV_{mi}/V_i(K_i/K_o + V_{mo}/V_{mi})$, where K_o and K_i are the probe binding constants to the external and internal vesicle interface, respectively (for a more detailed discussion see reference 18). As shown below, the ratio of the binding constants to each surface, K_i/K_o, is close to but not exactly 1 in these extruded vesicles.

pH dependence of the binding of trinitrophenols

The pH dependence of the binding of probes I and II was also investigated, and the data for probe I are shown in Fig. 7. The values of β remain constant at pH values lower than $\approx$7.8 but decrease at higher pHs with an apparent pK_a of $\sim$8.5. The absorbance of this probe also can be titrated in this range (see synthesis above) and shows a change consistent with a pK_a of $\sim$8.5. We believe that this titration and shift in binding is due to deprotonation of the nitrogen on the para position of the trinitrophenolate. In support of this notion is the fact that the nitrogen on di-1-(2,3,5 trinitrobenzene)amine (Dipicrylamine) has a pK_a below 3 (35). In addition, the diminished binding above pH = 8.5 is consistent with the larger electrostatic energy that a divalent species would experience in the membrane interface. In the experiments carried out here, measurements on membrane potentials were carried out below a pH of 7.5.

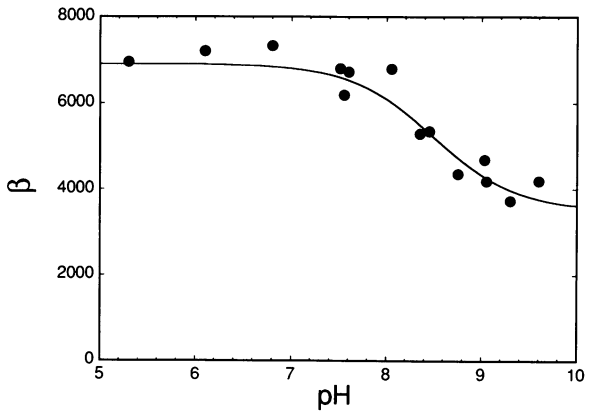

FIGURE 7 A plot of β for probe I in EPC vesicles as a function of pH. The values of β are obtained from the binding curves for probe I, such as those shown in Fig. 2, at a probe concentration of 5 μM. The binding constant titrates with an apparent pK of 8.5 and is apparently due to the deprotonation of the nitrogen linked to the para position on the ring.

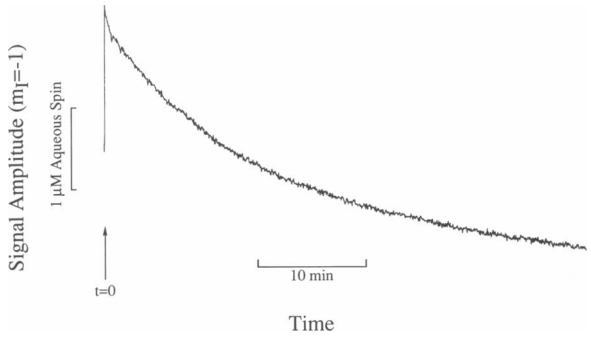

FIGURE 8 Time-dependence of the high-field signal of probe II when mixed with vesicles of EPC ($\sim$1.5 mg/ml) in the EPR spectrometer. The decay in the free signal provides a direct measure of the crossing rate of the probe and yields a value of 4×10^{-3} s^{-1}. The decay of the signal for probe I is faster than can be resolved by the EPR spectrometer, <10 ms. From the amplitude of this decay for II, the ratio of internal to external binding constants can be obtained (see text).

The transmembrane migration rates of TNP probes

The transmembrane migration rates for paramagnetic hydrophobic ions can be determined by monitoring their phase partitioning after rapid mixing with lipid vesicles (22). A time-dependent increase in binding is observed as a result of the additional membrane area that is available on the inner surface of the vesicle. Both the TNP probes I and II were examined to determine their rate of membrane crossing using a stopped-flow EPR spectrometer described elsewhere (22). Shown in Fig. 8 is a recording of the time dependence of the high-field resonance after the rapid mixing of II to lipid vesicles in the EPR spectrometer. The rate of membrane crossing is quite slow with a rate constant of $4.1 \pm 1.2 \times 10^{-3}$ s^{-1}. This rate constant is not significantly different than those found for many positive phosphonium ions (see Discussion below). Probe I, which lacks the additional hydroxyl, migrates much more rapidly. In mixing experiments that can resolve processes slower than 10 ms, no relaxation can be detected, and the rate constant for the transmembrane migration of probe I appears to be $\geq$1,000 times larger than that for probe II.

From relaxation data such as that shown in Fig. 8, the ratio of the internal to external probe binding constants, K_i/K_o, can be determined (36). This ratio is related to the

phase partitioning at $t = 0$, $\lambda(0)$ (when the probe has equilibrated with the external surface only) and the phase partitioning at $t = \infty$, $\lambda(\infty)$ (when the probe has equilibrated with both surfaces) by (37):

$$\frac{K_i}{K_o} = \left(\frac{V_{mo}}{V_{mi}}\right)\left[\left(\frac{V_i}{V_o} + 1\right)\left(\frac{\lambda(\infty)}{\lambda(0)}\right) - 1\right]. \quad (4)$$

Taking data such as that shown in Fig. 8, the ratio of K_i/K_o for probe II is found to be 1.14 ± 0.1 in these vesicle systems. Because probe I has a similar structure to probe II, this ratio will be used in the analysis of both probes I and II that is described below.

A simple thermodynamic model accounts for the voltage-dependent binding of spin-labeled TNP probes

Probes I and II both show a voltage-dependent partitioning in lipid vesicle systems. To establish the mechanism for the voltage dependence, the phase partitioning was compared with the expectations of a simple thermodynamic model previously shown to account for the voltage-dependent partitioning of hydrophobic cations (20). Within the framework of this model, the expected phase partitioning as a function of voltage is given as

$$\frac{N_b}{N_f} = K_o \frac{V_{mi}}{V_i}\left[\frac{\frac{K_i}{K_o} e^{\alpha zF\Delta\psi/RT} + \frac{V_{mo}}{V_{mi}} e^{zF(1-\alpha)\Delta\psi/RT}}{1 + \frac{V_o}{V_i} e^{zF\Delta\psi/RT}}\right] \quad (5)$$

Here, the parameter α represents the fraction of the applied membrane potential difference that exits across the binding sites of the ion, in other words, $\psi_{mo} = \alpha\Delta\psi$ and $\psi_{mi} = (1 - \alpha)\Delta\psi$. The inclusion of this parameter allows for the possibility that a fraction of the applied potential will fall between the membrane surface and the interfacial region where these hydrophobic anions bind. To determine the expected behavior of I as a function of $\Delta\psi$, the ratios V_o/V_i and V_{mo}/V_{mi} are determined from the vesicle concentration and vesicle size as described previously (20). With a value for K_i/K_o (obtained from the data in Fig. 8 and Eq. 4), the collection of terms, K_oV_{mi}/V_i, can be determined from the binding of the probe at zero potential. Using these parameters, experimentally determined phase partitioning as a function of transmembrane potential was compared with the voltage-dependence predicted by Eq. 5 at several values of α.

Shown in Fig. 9, *A* and *B* is the expected voltage-dependent partitioning for probes I and II, respectively, along with the experimental values. The experimental value for $\Delta\psi$ is determined from the buffer concentration and the internal vesicle pH according to Eq. 1. As seen in Fig. 9, excellent agreement between the experimentally determined partitioning and the expectations of Eq. 5 are obtained for values of α near 0.1. Also shown are the expected curves for $\alpha = 0.0$.

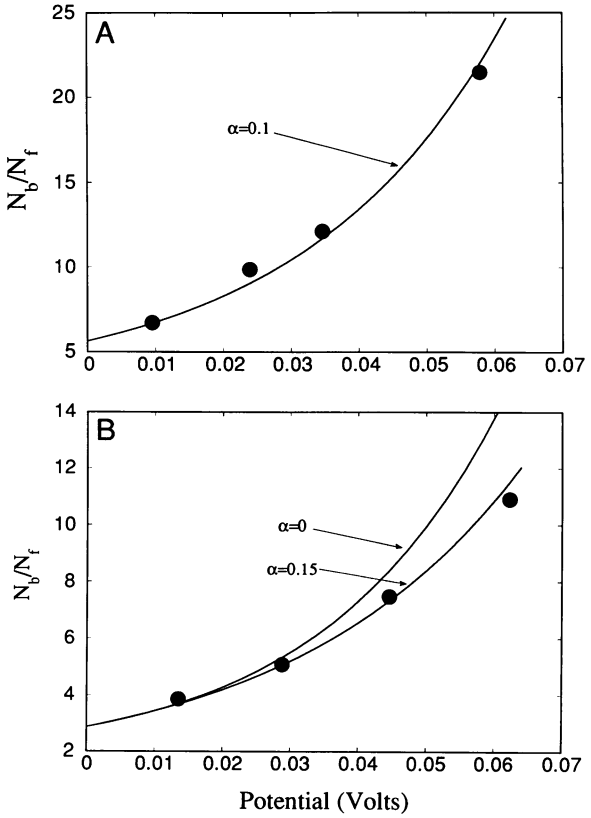

FIGURE 9 A comparison of the experimental voltage-dependent partitioning (●) for (*A*) probe I and (*B*) probe II with the predictions (*solid line*) of a simple thermodynamic model for hydrophobic ion equilibration across a vesicle membrane (see Eq. 5). The data are well accounted for by the model when α is ~0.1 for I and 0.15 for II (α is the only adjustable parameter in this model).

Effect of surface potential on the binding of I to bilayers

The TNP spin probes should partition to the surface of the membrane as charged species. As a result, the phase partitioning of I or II must be dependent on the membrane surface potential as well as the transmembrane potential. In the presence of surface potentials, the apparent binding constants become $K'_{i,o} = K_{i,o} \exp(zF\psi_{i,o}/RT)$, where $\psi_{i,o}$ are the internal and external vesicle surface potentials and $K_{i,o}$ are the internal and external binding constants in the presence of the potentials. To examine the behavior of the TNP probe in the presence of a surface potential, the slope of the binding curve, β, was measured for probe I in membranes composed of pure PC and PC plus negatively charged PS. The analysis carried out here assumes that changes in the binding of I as a function of PS are purely electrical in origin, an assumption that holds true for other charged amphiphilic probes in PC/PS membranes (37–39). In this case, the ratio of the slopes can be used to determine the surface potential according to $\psi_s = -(RT/F) \ln(\beta/\beta_o)$, where β_o is the slope of the binding curve for the uncharged PC membrane.

Shown in Fig. 10 are the experimentally determined

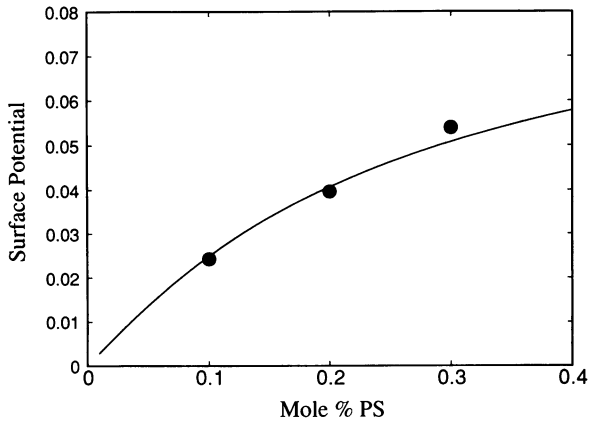

FIGURE 10 Surface potentials measured using the TNP based probe I in vesicles containing 0.1, 0.2 and 0.3 mole% phosphatidylserine. Lipid vesicles are formed in 100 mM NaCl, 5 mM ACES buffer, pH = 6.28. The potentials are determined from the slopes of the binding curves in the presence and absence of PS (see text). The solid line represents the predictions of the Gouy-Chapmann-Stern model with an ion binding constant for sodium of 0.75 M.

surface potentials determined using probe I, along with the behavior expected based on the Gouy-Chapman-Stern model. This model accurately accounts for the partitioning of other amphiphilic probes onto charged surfaces containing monovalent lipid (7, 40). As indicated in Fig. 10, this model also accurately predicts the binding changes measured for the negatively charged probe I in the presence of PS containing membranes. These data provide strong evidence that these probes interact with membranes as monovalent species.

Spin-labeled TNP probes transit vesicle bilayers in a charged state

The fact that probes I and II show potential-dependent equilibria (Figs. 3 and 9) indicates that they cross the membrane in an ionized form. Further evidence regarding this point was obtained by examining the effect of phloretin on the transmembrane migration rate of II in vesicles. Phloretin reduces the magnitude of the membrane dipole potential, slowing the migration rate of anions and accelerating the migration rate of cations in planar bilayers as well as vesicles (41–43). The effect of phloretin on the translocation rate of II is shown in Table 1. Phloretin slows the rate of migration of probe II, and the change is similar to that of phloretin on the migration of other monovalent hydrophobic anions in lipid vesicles (Franklin, J. C., and D. S. Cafiso, manuscript in preparation) (43).

At pH values in the neighborhood of their pK, certain weak acids and bases act as protonophores. For example, 2,4 dinitrophenol (pK_a = 4) (44) is a well-known uncoupler of oxidative phosphorylation that carries protons because both its charged and uncharged forms are permeable and present near neutral pH (45). The pK_a of the phenolic group in I and II is unknown but is expected to be less than that of dinitrophenol due to the effect of the additional nitro substituent. This lower pK_a should reduce the protonophoric activity at neutral pH by reducing the concentration of the highly permeable uncharged form of TNP.

Although the activity of I or II as protonophores may depend on pH as well as their membrane concentrations, no evidence for a strong proton carrying activity of these probes was found in any of the measurements described above. When probes I or II were added to lipid vesicles containing pH gradients, their phase partitioning was not dependent on the pH gradient until after the addition of CCCP. This result indicates that over the time periods of these measurements (several minutes), protons are not brought to electrochemical equilibrium by these TNP derivatives. In other words, the rapid establishment of a membrane potential required the addition of CCCP. From this observation, we conclude that I and II are not potent protonophores and that the transmembrane distribution of these probes responds to membrane potentials and not pH gradients.

DISCUSSION

The work presented here describes the synthesis and characterization of a new class of hydrophobic ion spin-labels based on the trinitrophenolate anion. These spin-labeled anions exhibit a voltage-dependent phase partitioning in vesicles that can be accounted for by a simple thermodynamic model, thereby allowing the quantitation of potentials directly from their EPR spectra. Several important considerations inspired the development of these probes. First, they are expected to transit membranes at a much more rapid rate than hydrophobic cations, providing a tool to monitor rapid potential changes across vesicles. Indeed, the TNP derivative I should respond to transmembrane potential changes that occur within the millisecond time range. Second, these anion probes, when used in combination with hydrophobic cations, provide a powerful approach to probe the electrostatic potential in the membrane interior. These potentials will

TABLE 1 Effect of phloretin on the forward rate constant for transmembrane crossing of the trinitrophenol nitroxide II in EPC vesicles

Mol% phloretin	k_i
0	$3.3 \pm 0.2 \times 10^{-3}\ s^{-1}$
3.6	$2.4 \pm 0.2 \times 10^{-3}\ s^{-1}$
7.1	$0.97 \pm 0.2 \times 10^{-3}\ s^{-1}$

The inward rate constant for the transmembrane migration of II was determined following a procedure used previously to determine the rate constant for spin-labeled phosphoniums.[22] Phloretin was incorporated into the vesicles by dissolving the lipid with phloretin before removing the organic solvent (see Experimental). Following extrusion and centrifugation, phloretin was present at the level indicated in the vesicle membrane.

be important for investigating processes such as protein insertion into membranes and voltage-dependent conformational events in membrane proteins. Finally, these anion probes are most sensitive to inside positive potentials in vesicles, potentials that are not measured accurately by hydrophobic cations. They will be a useful tool in systems such as reconstituted bacteriorhodopsin, where light-generated potentials are inside positive.

Positively charged phosphonium ions have a half-time for transmembrane equilibration in EPC vesicles of ~700 s (22). Because the membrane dipole potential (Fig. 1) produces a difference of 7–8 kcal/mol in activation energy between cations and anions (17), hydrophobic ions like I are expected to have half-times for equilibration of a few milliseconds. This is consistent with the experimental result that the half-time for I is less than the 10-ms time resolution of the rapid mixing system used here.

The anion probe I has a binding constant that is ~500–1,000 times larger than positively charged triarylalkylphosphoniums (20), and this increased binding is also an expected consequence of the dipole potential. The free energy of binding (ΔG_B^0) for I is 3.5–4 kcal/mol more negative than these positive phosphoniums, despite the additional hydrophobicity of the positively charged probe. Given the differences in structure between these probes, these values are not inconsistent with the 5 kcal/mol difference between the binding energies of tetraphenylphosphonium and tetraphenylborate (19). Thus, the TNP probe I appears to behave as expected for a hydrophobic anion. Taken together with the voltage-dependent phase partitioning and phloretin-sensitive transport rates, this is strong evidence that these new anion probes transit and associate with membranes in a charged form.

As a result of the strong binding that I exhibits to the membrane interface, II was synthesized with the expectation that its additional hydrophilicity would lower the affinity of the probe for the membrane/solution interface. This is indeed the case, and II has a free energy of binding (ΔG_B^0) ~1 kcal/mol more positive than that of I. The hydroxyl group in II is almost certainly hydrogen bonded to solvent when it is in the aqueous phase, and it must also be participating in a hydrogen bond when it is membrane bound. If this were not the case, then a much weaker binding of II would be expected. The axial rotation rate of II is also an order of magnitude slower than that of I, even though these probes are of similar size. This is consistent with the idea that the hydroxyl group in II participates in a hydrogen bond within its membrane binding domain. In contrast to I, the transmembrane migration rate of II is surprising slow. This probe experiences an energy barrier that is ~5 kcal/mol larger than that for probe I, and its crossing rate is comparable with that for many hydrophobic cations. Again, this finding is consistent with the idea that II has additional interactions within its membrane binding site compared with I, and the magnitude of the activation energy difference is close to that expected for a hydrogen bond in a hydrophobic environment.

The slow migration rate observed for II indicates that it will not be a useful probe for rapid changes in membrane potentials; however, its slow migration rate does facilitate certain measurements. Because its migration rate is slow, it is readily determined, providing a convenient way to probe the energy barrier for anion transport through bilayers. This probe can be used readily to quantitate changes in the energy barrier for anion transport that result from changes in the membrane dipole potential (Franklin, J. C., and D. S. Cafiso, manuscript in preparation).

The physical basis for the voltage-dependent binding of probes I and II shown in Figs. 3 and 9 is the difference in the membrane surface to aqueous volume ratio between the inside and outside of a lipid vesicle. As a result of this difference, the accumulation of probes I or II on the vesicle interior (e.g., in response to an positive inside potential) leads to an increase in partitioning to the membrane phase. This mechanism is identical to that described previously for spin-labeled phosphonium ions (18). To exploit this mechanism, these probes must be used at lipid concentrations that permit a measurable partitioning between membrane and aqueous phases. For the negatively charged probes described here, these lipid concentrations are much lower than those used for positive probes of comparable hydrophobicity. This is a result of the much more negative ΔG_B^0 of the anion probes. To maintain a probe-to-lipid ratio that is nonperturbing, the anion probes were used here at lower concentrations than those used previously for positively charged hydrophobic ion probes. Fortunately, because of the high sensitivity of EPR, it has generally been possible to find experimental conditions where these probes partition at low probe-to-lipid ratios.

The synthesis and voltage dependence of TNP-based probes has not been described previously. However, spin-labels based on dinitrophenol have been synthesized (46, 47). To our knowledge, the voltage-dependence of these derivatives has not been characterized, and they also could be useful probes of membrane potential. However, the absence of a third nitro group would be expected to raise the pK_a of the phenolic group, and this should place a larger fraction of the probe in a protonated form. Dinitrophenol is a protonophore, and the spin-labeled derivative of this molecule also may have protonophoric activity (45).

In the analysis of the binding of probes I and II to vesicles formed by extrusion, the binding of the probe to the internal membrane interface is found to be slightly larger than to the external interface. A difference in binding between internal and external vesicle surfaces is not unreasonable, given the lipid packing asymmetry found in small vesicles (48). In fact, similar differences were observed for phosphoniums in sonicated vesicles (49).

Taking the values of K_i/K_o obtained from the data in Fig. 8, the potential dependent partitioning in Fig. 9 is fit best when α is $\sim$0.1. A non-zero value for α is not physically unreasonable. It implies that a portion of the membrane potential drops between the membrane surface and the region where these hydrophobic ions bind near the level of the carbonyl oxygens (9). Indeed, for the well-characterized hydrophobic anion tetraphenylborate, a value of $\alpha \cong 0.12$ is found from planar bilayer work (14).

In summary, a new series of spin-labeled hydrophobic anion probes has been synthesized and characterized in lipid vesicle systems. These probes exhibit a transmembrane potential-dependent phase partitioning that can be accounted for using a simple thermodynamic model that previously accounted for the behavior of spin-labeled phosphoniums. These probes provide a new tool that can be used to quantitate rapid changes in membrane potential and examine the internal electrostatic potentials of membranes.

This work was supported by National Institutes of Health (NIH) grant GM-35215 and National Science Foundation grant BNS 8908692 to D. S. Cafiso and by NIH grant EY-05216 and the Jules Stein Professorship to W. L. Hubbell. J. C. Franklin received support from an NIH training grant GM-08323 in molecular biophysics to the University of Virginia during the course of this work.

Received for publication 16 September 1992 and in final form 9 November 1992.

REFERENCES

1. Kim, J., M. Mosior, L. Chung, H. Wu, and S. McLaughlin. 1990. Binding of peptides with basic residues to membranes containing acidic phospholipids. *Biophys. J.* 60:135–148.
2. Hartmann, E., T. A. Rapoport, and H. F. Lodish. 1989. Predicting the origin of eukaryotic membrane spanning proteins. *Proc. Natl. Acad. Sci. USA.* 86:5786–5790.
3. Dalbey, R. E. 1990. Positively charged residues are important determinants of membrane protein topology. *Trends Biochem. Sci.* 15:253–257.
4. Andersson, H., E. Bakker, and G. Von Heijne. 1992. Different positively charged amino acids have similar effects on the topology of a polytopic transmembrane protein in *Escherichia coli*. *J. Biol. Chem.* 267:1491–1495.
5. Cafiso, D. S. 1991. Lipid bilayers: membrane-protein electrostatic interactions. *Curr. Opin. Struct. Biol.* 1:185–190.
6. McLaughlin, S. 1977. Electrostatic potentials at membrane solution interfaces. *Curr. Top. Membr. Transp.* 9:71–144.
7. McLaughlin, S. A. 1989. The electrostatic properties of membranes. *Annu. Rev. Biophys. Biophys. Chem.* 18:113–136.
8. Honig, B. H., W. L. Hubbell, and R. F. Flewelling. 1986. Electrostatic interactions in membranes and proteins. *Annu. Rev. Biophys. Biophys. Chem.* 15:163–193.
9. Ellena, J. F., R. N. Dominey, S. J. Archer, Z.-C. Zu, and D. S. Cafiso. 1987. The localization of hydrophobic ions in phospholipid bilayers using ^{1}H nuclear Overhauser effect spectroscopy. *Biochemistry.* 26:4584–4592.
10. Simon, S. A., C. A. Fink, A. K. Kenworthy, and T. J. McIntosh. 1991. The hydration pressure between lipid bilayers. Comparison of measurements using x-ray diffraction and calorimetry. *Biophys. J.* 59:538–564.
11. Gawrisch, K., D. Ruston, J. Zimmerberg, V. A. Parsegian, R. P. Rand, and N. Fuller. 1992. Membrane dipole potentials, hydration forces and the ordering of water at membrane interfaces. *Biophys. J.* 61:1213–1223.
12. Cafiso, D. S., and W. L. Hubbell. 1980. Light-induced interfacial potentials in photoreceptor membranes. *Biophys. J.* 30:243–264.
13. Ketterer, B., B. Neumcke, and P. Lauger. 1971. Transport mechanism of hydrophobic ions through lipid bilayer membranes. *J. Membr. Biol.* 5:225–245.
14. Andersen, O. S., and M. Fuchs. 1975. Potential energy barriers to ion transport within lipid bilayers. *Biophys. J.* 15:795–829.
15. Andersen, O. S., S. Feldberg, H. Nahadoman, S. Levy, and S. McLaughlin. 1978. Electrostatic interactions among hydrophobic ions in lipid bilayer membranes. *Biophys. J.* 21:35–70.
16. Lauger, P., R. Benz, G. Stark, E. Bamberg, P. C. Jordan, A. Fahr, and W. Brock. 1981. Relaxation studies of ion transport systems in lipid bilayer membranes. *Q. Rev. Biophys.* 14:513–598.
17. Flewelling, R. F., and W. L. Hubbell. 1986. The membrane dipole potential in a total membrane potential model. Applications to hydrophobic ion interactions with membranes. *Biophys. J.* 49:541–552.
18. Cafiso, D. S., and W. L. Hubbell. 1981. ESR determination of membrane potentials. *Annu. Rev. Biophys. Bioeng.* 10:217–244.
19. Flewelling, R. F., and W. L. Hubbell. 1986. Hydrophobic interactions within membranes. Thermodynamic analysis of tetraphenylphosphonium binding to vesicles. *Biophys. J.* 49:531–540.
20. Cafiso, D. S., and W. L. Hubbell. 1978. Estimation of transmembrane potentials from phase equilibria of hydrophobic paramagnetic ions. *Biochemistry.* 17:187–195.
21. Liberman, E. A., and V. A. Topaly. 1968. Selective transport through bimolecular phospholipid membranes. *Biochim. Biophys. Acta.* 163:125–136.
22. Cafiso, D. S., and W. L. Hubbell. 1982. Transmembrane electrical currents of spin-labeled hydrophobic ions. *Biophys. J.* 39:263–272.
23. Hubbell, W. L., W. Froncisz, and J. S. Hyde. 1987. A continuous stopped flow EPR spectrometer based on a loop gap resonator. *Rev. Sci. Instrum.* 58:1879–1886.
24. Singleton, W. S., M. S. Gray, M. L. Brown, and J. L. White. 1965. Chromatographically homogeneous lecithin from egg phospholipids. *J. Am. Oil Chem. Soc.* 42:53–56.
25. Bartlett, G. R. 1959. Phosphorous assay in column chromatography. *J. Biol. Chem.* 234:466–468.
26. Archer, S. J., and D. S. Cafiso. 1991. A voltage-dependent conductance for alamethicin in phospholipid vesicles: a test for the mechanism of gating. *Biophys. J.* 60:380–388.
27. Montal, M., and P. Mueller. 1972. Formation of biomolecular membranes from lipid monolayers and a study of their electrical properties. *Proc. Natl. Acad. Sci. USA.* 69:3561–3566.
28. Meirovitch, E., D. Igner, E. Igner, G. Moro, and J. H. Freed. 1982. Electron-spin relaxation and ordering in smectic and supercooled nematic liquid crystals. *J. Chem. Phys.* 77:3915–3938.
29. Schneider, D. J., and J. H. Freed. 1989. Calculating slow motional magnetic resonance spectra. A users guide. *In* Spin Labeling, Theory and Applications. Vol. 8. L. J. Berliner, editor. Plenum, New York. 1–76.
30. Still, W. C., M. Kahn, and A. Mitra. 1978. Rapid chromatographic technique for preparative separations with moderate resolution. *J. Org. Chem.* 43:2923–2925.
31. Corey, E. J., and M. Chaykovsky. 1965. Dimethyloxosulfonium methylide ($(CH_3)_2SOCH_2$) and dimethylsulfonium methylide ($(CH_3)_2SCH_2$). *J. Am. Chem. Soc.* 87:1353–1364.

32. Rauchman, E. J., G. M. Rosen, and M. B. Abou-Donia. 1976. The use of trimethylsulfonium iodide in the synthesis of biologically active nitroxides. *Org. Prep. Proced.* 8:159–161.

33. McManus, S. P., C. A. Larson, and R. A. Hearn. 1973. The synthesis of aminoalcohols from ammonia. *Synth. Commun.* 3:177–180.

34. Huang, C. 1969. Studies on phosphatidylcholine vesicles. Formation and physical characteristics. *Biochemistry.* 8:334–351.

35. Benz, R., and B. F. Gisin. 1978. Influence of membrane structure on ion transport through lipid bilayer membranes. *J. Membr. Biol.* 40:293–314.

36. Sundberg, S. A., and W. L. Hubbell. 1986. Investigation of surface potential asymmetry in phospholipid vesicles by a spin-label relaxation method. *Biophys. J.* 49:553–562.

37. Hartsel, S. C., and D. S. Cafiso. 1986. A test of discreteness-of-charge effects in phospholipid vesicles: measurements using paramagnetic amphiphiles. *Biochemistry.* 25:8214–8219.

38. Cafiso, D., A. McLaughlin, S. McLaughlin, and A. Winiski. 1989. Measuring electrostatic potentials adjacent to bilayer membranes. *Methods Enzym.* 171:342–364.

39. Winiski, A. P., A. C. McLaughlin, R. V. McDaniel, M. Eisenberg, and S. McLaughlin. 1986. An experimental test of the discreteness-of-charge effect in positive and negative lipid bilayers. *Biochemistry.* 25:8206–8214.

40. Langer, M., D. Cafiso, S. Marcelja, and S. McLaughlin. 1990. Electrostatics of phosphoinositide bilayer membranes: theoretical and experimental results. *Biophys. J.* 57:335–349.

41. Andersen, O. S., A. Finkelstein, I. Katz, and A. Cass. 1976. Effect of phloretin on the permeability of thin lipid membranes. *J. Gen. Physiol.* 67:749–771.

42. Melnik, E., R. Latorre, J. Hall, and D. Tosteson. 1977. Phloretin induced changes in ion transport across lipid bilayer membranes. *J. Gen. Physiol.* 69:243–257.

43. Perkins, W. R., and D. S. Cafiso. 1987. A procedure using voltage-sensitive spin-labels to monitor dipole potential changes in phospholipid vesicles: the estimation of phloretin-induced conductance changes in vesicles. *J. Membr. Biol.* 96:165–173.

44. Fugita, T. 1966. The analysis of physiological activity of substituted phenols with substitutent constants. *J. Med. Chem.* 9:797–803.

45. McLaughlin, S., and J. Dilger. 1980. The transport of protons across membranes by weak acids. *Physiol. Rev.* 60:825–863.

46. Chen, W. L., and J. C. Hsia. 1974. Studies on motional characteristics and distribution of protonated and anionic forms of spin-labeled 2,4,-dinitrophenol in phospholipid bilayer membranes. *Biochemistry.* 13:4948–4952.

47. Hankovszky, H. O., K. Hideg, and M. J. Lovas. 1989. Synthesis and reaction of ortho-fluoronitroaryl nitroxides. Novel versatile synthons and reagents for spin-labelling studies. *Can. J. Biochem.* 67:1392–1400.

48. Huang, C., and J. T. Mason. 1978. Geometric packing constraints in egg phosphatidylcholine vesicles. *Proc. Natl. Acad. Sci. USA.* 75:308–310.

49. Raines, D. E., and D. S. Cafiso. 1984. Potential-dependent phase partitioning of fluorescent hydrophobic ions. *J. Membr. Biol.* 82:241–247.

50. Pasenkiewicz-Gierula, M., J. S. Hyde, and J. R. Pilbrow. 1983. Simulation of Q-band ESR spectra of immobilized spin-labels. *J. Magn. Res.* 55:255–265.